PROCEEDINGS OF SPIE

Infrared Technology and Applications XXXIII

Bjørn F. Andresen
Gabor F. Fulop
Paul R. Norton
Editors

9–13 April 2007
Orlando, Florida, USA

Sponsored and Published by
SPIE—The International Society for Optical Engineering

Volume 6542
Part One of Two Parts

The International Society for Optical Engineering

Proceedings of SPIE—The International Society for Optical Engineering, 9780819466648, v. 6542

SPIE is an international technical society dedicated to advancing engineering and scientific applications of optical, photonic, imaging, electronic, and optoelectronic technologies.

The papers included in this volume were part of the technical conference cited on the cover and title page. Papers were selected and subject to review by the editors and conference program committee. Some conference presentations may not be available for publication. The papers published in these proceedings reflect the work and thoughts of the authors and are published herein as submitted. The publisher is not responsible for the validity of the information or for any outcomes resulting from reliance thereon.

Please use the following format to cite material from this book:
Author(s), "Title of Paper," in *Infrared Technology and Applications XXXIII*, edited by Bjørn F. Andresen, Gabor F. Fulop, Paul R. Norton, Proceedings of SPIE Vol. 6542 (SPIE, Bellingham, WA, 2007) Article CID Number.

ISSN 0277-786X
ISBN 9780819466648

Published by
SPIE
P.O. Box 10, Bellingham, Washington 98227-0010 USA
Telephone +1 360 676 3290 (Pacific Time) · Fax +1 360 647 1445
SPIE.org

Printed in the United States of America.

Publication of record for individual papers is online in the SPIE Digital Library.

SPIE Digital Library

SPIEDigitalLibrary.org

Paper Numbering: Proceedings of SPIE follow an e-First publication model, with papers published first online and then in print and on CD-ROM. Papers are published as they are submitted and meet publication criteria. A unique, consistent, permanent citation identifier (CID) number is assigned to each article at the time of the first publication. Utilization of CIDs allows articles to be fully citable as soon they are published online, and connects the same identifier to all online, print, and electronic versions of the publication. SPIE uses a six-digit CID article numbering system in which:

- The first four digits correspond to the SPIE volume number.
- The last two digits indicate publication order within the volume using a Base 36 numbering system employing both numerals and letters. These two-number sets start with 00, 01, 02, 03, 04, 05, 06, 07, 08, 09, 0A, 0B … 0Z, followed by 10-1Z, 20-2Z, etc.

The CID number appears on each page of the manuscript. The complete citation is used on the first page, and an abbreviated version on subsequent pages. Numbers in the index correspond to the last two digits of the six-digit CID number.

Contents

Part One

SHORT-WAVE IR FPAs

QDIP FPA ADVANCES

QWIP FPAs AND APPLICATIONS

DEVELOPMENT OF TECHNOLOGIES FOR 3RD-GENERATION IR IMAGERS I

DEVELOPMENT OF TECHNOLOGIES FOR 3RD-GENERATION IR IMAGERS II

DEVELOPMENT OF 3RD-GENERATION IR IMAGERS AND THEIR TECHNOLOGIES

NOVEL UNCOOLED TECHNOLOGIES I

NOVEL UNCOOLED TECHNOLOGIES II

Part Two

UNCOOLED FPAs AND APPLICATIONS

INFRARED OPTICS AND APPLICATIONS

VIBRATION CONTROL AND STABILIZATION IN EO EQUIPMENT: JOINT SESSION WITH 6569

INFRARED IN FUTURE SOLDIER SYSTEMS

IRST/TARGET ACQUISITION: SYSTEMS AND TECHNOLOGIES I

SELECTED TECHNOLOGY PRESENTATIONS

Conference Committee

Symposium Chair

John C. Carrano, Luminex Corporation (USA)

Symposium Cochair

Larry B. Stotts, Defense Advanced Research Projects Agency (USA)

Program Track Chair

Gabor F. Fulop, Maxtech International Inc. (USA)

Conference Chairs

Bjørn F. Andresen, Elbit Systems Electro-Optics ElOp Ltd. (Israel)
Gabor F. Fulop, Maxtech International Inc. (USA)
Paul R. Norton, U.S. Army Night Vision & Electronic Sensors Directorate (USA)

Program Committee

Christopher C. Alexay, StingRay Optics, LLC (USA)
Raymond S. Balcerak, Defense Advanced Research Projects Agency (USA)
Stefan T. Baur, Raytheon Vision Systems (USA)
Philippe F. Bois, Thales Research and Technology (France)
Wolfgang A. Cabanski, AIM Infrarot-Module GmbH (Germany)
John T. Caulfield, Cyan Systems (USA)
Jean-Pierre Chatard, ULIS (France)
Peter N. J. Dennis, QinetiQ Ltd. (United Kingdom)
John W. Devitt, L-3 Communications Cincinnati Electronics, Inc. (USA)
Michael T. Eismann, Air Force Research Laboratory (USA)
Martin H. Ettenberg, Sensors Unlimited, Goodrich Corporation (USA)
Sarath D. Gunapala, Jet Propulsion Laboratory (USA)
Masafumi Kimata, Ritsumeikan University (Japan)
Hee Chul Lee, Korea Advanced Institute of Science and Technology (South Korea)
Paul D. LeVan, Air Force Research Laboratory (USA)
Wei Lu, Shanghai Institute of Technical Physics (China)
Mark A. Massie, Nova Sensors (USA)
Paul L. McCarley, Air Force Research Laboratory (USA)
R. Kennedy McEwen, SELEX Sensors and Airborne Systems Ltd. (United Kingdom)
Paul F. McManamon, Air Force Research Laboratory (USA)

John L. Miller, FLIR Systems, Inc. (USA)
A. Fenner Milton, U.S. Army Night Vision & Electronic Sensors Directorate (USA)
Ofer Nesher, SemiConductor Devices (Israel)
Peter W. Norton, BAE Systems North America (USA)
Francis P. Pantuso, U.S. Army Night Vision & Electronic Sensors Directorate (USA)
Herbert K. Pollehn, Army Research Laboratory (USA)
Ingmar G. E. Renhorn, Swedish Defence Research Agency (Sweden)
Antoni Rogalski, Wojskowa Akademia Techniczna (Poland)
Ingo Rühlich, AIM Infrarot-Module GmbH (Germany)
Myron J. Scholten, DRS Sensors & Targeting Systems, Inc. (USA)
Venkataraman S. Swaminathan, U. S. Army RDECOM-ARDEC (USA)
Meimei Z. Tidrow, Missile Defense Agency (USA)
Philippe M. Tribolet, Sofradir (France)
Jay Vizgaitis, U.S. Army Night Vision & Electronic Sensors Directorate (USA)
Kadri Vural, Teledyne Scientific Company (USA)

Session Chairs

1 Type II Superlattice FPAs
Meimei Z. Tidrow, Missile Defense Agency (USA)
Manijeh Razeghi, Northwestern University (USA)

2 Keynote Session
Gabor F. Fulop, Maxtech International, Inc. (USA)

3 HgCdTe
Philippe M. Tribolet, Sofradir (France)

4 Short-Wave IR FPAs
Martin H. Ettenberg, Sensors Unlimited, Goodrich Corporation (USA)

5 QDIP FPA Advances
Venkataraman S. Swaminathan, U.S. Army RDECOM-ARDEC (USA)

6 QWIP FPAs and Applications
Philippe F. Bois, Thales Research and Technology (France)
Sarath D. Gunapala, Jet Propulsion Laboratory (USA)

7 Development of Technologies for 3rd-Generation IR Imagers I
Paul R. Norton, U.S. Army Night Vision & Electronic Sensors Directorate (USA)
Paul L. McCarley, Air Force Research Laboratory (USA)
John T. Caulfield, Cyan Systems (USA)

8 Development of Technologies for 3rd-Generation IR Imagers II
Paul R. Norton, U.S. Army Night Vision & Electronic Sensors Directorate (USA)
Paul L. McCarley, Air Force Research Laboratory (USA)
John T. Caulfield, Cyan Systems (USA)

9 Development of 3rd-Generation IR Imagers and Their Technologies
Paul R. Norton, U.S. Army Night Vision & Electronic Sensors Directorate (USA)
Peter N. J. Dennis, QinetiQ Ltd. (United Kingdom)
R. Kennedy McEwen, SELEX Sensors and Airborne Systems Ltd. (United Kingdom)

10 Novel Uncooled Technologies I
Francis P. Pantuso, U.S. Army Night Vision & Electronic Sensors Directorate (USA)

11 Keynote Session
Bjørn F. Andresen, Elbit Systems Electro-Optics ElOp Ltd. (Israel)

12 Novel Uncooled Technologies II
Francis P. Pantuso, U.S. Army Night Vision & Electronic Sensors Directorate (USA)

13 Uncooled FPAs and Applications
Raymond S. Balcerak, Defense Advanced Research Projects Agency (USA)
Masafumi Kimata, Ritsumeikan University (Japan)
Jean-Luc Tissot, ULIS (France)

14 Infrared Optics and Applications
Christopher C. Alexay, StingRay Optics, LLC (USA)
Jay Vizgaitis, U.S. Army Night Vision & Electronic Sensors Directorate (USA)

15 Cryocoolers for Focal Plane Arrays
Ingo Rühlich, AIM Infrarot-Module GmbH (Germany)

16 Vibration Control and Stabilization in EO Equipment: Joint session with 6569
Alexander M. Veprik, Ricor Cryogenic and Vacuum Systems (Israel)
Dan C. Herrick, Air Force Research Laboratory Directed Energy Directorate (USA)

17 Infrared in Future Soldier Systems
Gabor F. Fulop, Maxtech International, Inc. (USA)
Gary L. Jinks, GLJ Group (USA)

18 IRST/Target Acquisition: Systems and Technologies I
Michael T. Eismann, Air Force Research Laboratory (USA)
Herbert K. Pollehn, Army Research Laboratory (USA)
Gil A. Tidhar, Optigo Systems, Ltd. (Israel)

19 IRST/Target Acquisition: Systems and Technologies II
Gil A. Tidhar, Optigo Systems, Ltd. (Israel)
Michael T. Eismann, Air Force Research Laboratory (USA)
Herbert K. Pollehn, Army Research Laboratory (USA)

20 Selected Application Presentations
John L. Miller, FLIR Systems, Inc. (USA)

21 Selected Technology Presentations
John L. Miller, FLIR Systems, Inc. (USA)

22 ROIC and Non-uniformity Correction
Ingmar G. E. Renhorn, Swedish Defence Research Agency (Sweden)

Introduction

The Thirty-Third conference on Infrared Technology and Applications was held the week of April 9-13, 2007 at the Orlando World Center Marriott Resort and Convention Center in Orlando, Florida. The agenda was divided into 22 sessions:

1. Type II superlattice FPAs
2. Keynote—IR material research at the Army Research Laboratory
3. HgCdTe
4. Short-wave IR FPAs
5. QDIP FPA advances
6. QWIP FPAs and applications
7. Development of technologies for 3rd generation IR imagers I
8. Development of technologies for 3rd generation IR imagers II
9. Development of 3rd generation IR imagers and their technologies
10. Novel uncooled technologies I
11. Keynote— HgCdTe on low-cost substrates (SWIR to LWIR): opportunities, challenges, and innovations
12. Novel uncooled technologies II
13. Uncooled FPAs and applications
14. Infrared optics and applications
15. Cryocoolers for focal plane arrays
16. Joint session with DSS 6569: Vibration control and stabilization in EO equipment
17. Infrared in future soldier systems
18. IRST/target acquisition: systems and technologies I
19. IRST/target acquisition: systems and technologies II
20. Selected application presentations
21. Selected technology presentations
22. ROIC and non-uniformity correction

In addition, there were approximately ten poster papers presented for discussion on Thursday evening. Highlights of each session are noted below. Papers cited are referenced as "*-xx*" where the numbers refer to the paper number in the Proceedings, for example *6542-xx*.

1. Type II superlattice FPAs

Type II superlattice detectors (T2SL), also known as strained-layer superlattices (SLS) are a potential replacement for HgCdTe detectors. Like HgCdTe they have a direct bandgap and a high absorption coefficient α, that allows the detector layer to be thin. Unlike QWIP devices, normally-incident radiation is absorbed, so that grating structures are not needed. The most popular material for making T2SL devices is the combination of GaSb and InAs layers on GaSb substrates. Focal planes in both MWIR and LWIR have been demonstrated in recent years. This session updates the progress in this material system.

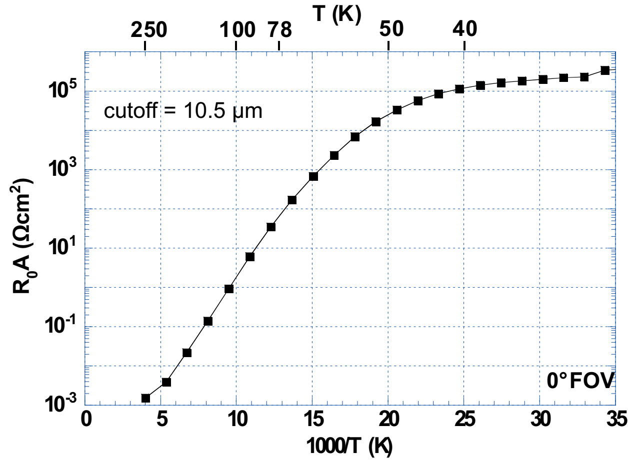

Fig. 1 R_0A vs 1/T for an LWIR type II superlattice described in paper -01.

Paper -01 describes efforts at Raytheon and the Jet Propulsion Laboratory to develop LWIR devices. Mesa structures were fabricated from InAs/GaSb layers grown on GaSb in a 256^2 format with 30 µm pixels. The p-i-n diodes were passivated with SiO_2. To minimize absorption the GaSb substrate was thinned to 90 µm. At 77 K the cutoff was 10.5 µm with R_0A values in the range of 4-30 Ωcm^2 as illustrated in Fig. 1. Maximum R_0A as high as 10^5 Ωcm was observed, limited by tunneling for T<56 K. Imaging was demonstrated.

W-structured type II superlattice LWIR diodes were described in paper -02 by the Naval Research Laboratory. An additional control parameter is available in the W-structure. The key feature of this structure is a graded bandgap combined with shallow mesa etching that does not expose mesa sidewalls in the narrow-bandgap region. LWIR diode R_0A values for these devices were about 10× lower than HgCdTe as shown in Fig. 2. Surface passivation experiments were reviewed.

Paper -03 summarizes work on LWIR type II superlattices at Northwestern University. They showed that quantum efficiency rose to as much as 54% with a 6 µm absorption layer. An average R_0A value of 13 Ωcm^2 was achieved for a cutoff of 12 µm. 320×256 FPAs were fabricated with 25 µm pixels and showed high operability.

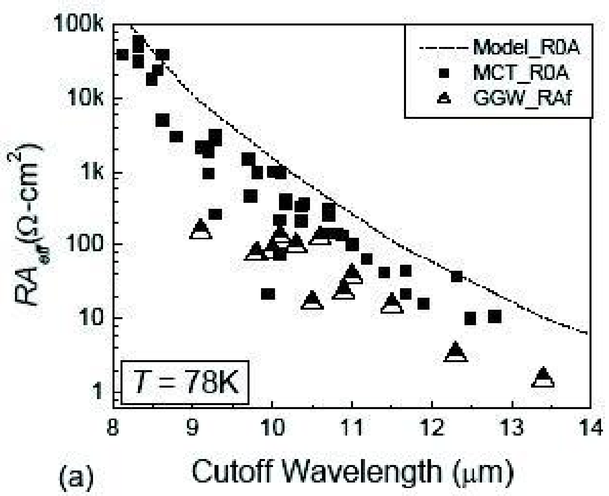

Fig. 2 R_0A vs cutoff wavelength for W-structured type II superlattices described in paper -02 compared to HgCdTe diodes.

Type II superlattice detectors spanning SWIR/MWIR (3.7 μm), and LWIR (10.3 and 12 μm) were described in paper -04 by the Jet Propulsion Laboratory. Experiments with p-i-n diodes on GaSb substrates were carried out, varying the layer interface between Ga-As and In-Sb. D* values for the 3.7 μm cutoff devices were reported to be as high as 8×10^{13} Jones. R_0A values for the 10.2 and 12 μm cutoff samples were 40 and 5 Ωcm^2, respectively. Passivation issues were also addressed.

Papers -05 and -06 were presented by the Fraunhofer Institute and AIM. They are focused on developing two-color MWIR T2SL devices for threat warning. Updates were given on single-color detectors that have been reported in previous years, now with 24 μm pixel pitch in a 384×288 format having NEΔT of 28 mK at f/2.4 with a 4.9 μm cutoff and 1 msec integration time. Dual color MWIR devices are being developed on a 40 μm pitch with three indium bumps per pixel (see Fig. 3), with plans to shrink the pixels to 30 μm in the future using a two-bump per pixel design that is slated for deployment on military transports. Development of LWIR T2SL detectors are planned.

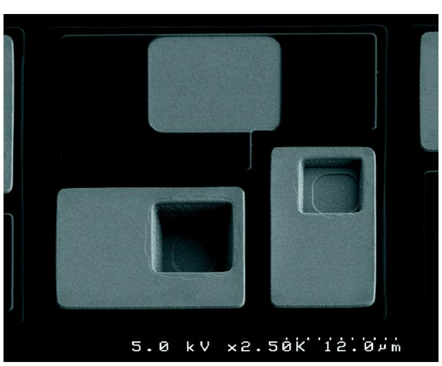

Fig. 3 Two-color T2SL detector described by AIM and Fraunhofer in papers -05 and -06. Each pixel has 3 indium bumps.

High operating temperature MWIR detector development using T2SL detectors is the goal of the University of New Mexico and Santa Barbara Focalplane as described in paper -07. Devices were fabricated on GaSb substrates with p-on-n polarity. Variable-area diodes were measured between 82 and 240 K, with R_0A values of ~10^5 and 0.24 Ωcm^2, and D*s of 2×10^{12} and 2×10^9 Jones, respectively. SiN_x deposition at room temperature was found to be an effective passivation. A new detector type, n-B-n, where B is a barrier, was briefly described along with initial experiments for growth on GaAs substrates.

A review of the basic properties and attractive features of T2SL detectors was presented in paper -08 by Kirtland Air Force Base and Northwestern University. Modeling and the growth of a new “M” structure was reviewed, along with experimental results from device measurements and imaging experiments.

Modeling of the system interface and application was the subject of paper -09 by BAE Systems. A general overview of the scope of considerations was given that may be applicable to all detector types.

Teledyne, the Naval Research Laboratory and Northwestern University compared HgCdTe and T2SL approaches in paper -10. The state-of-the-art of HgCdTe was reviewed and results for T2SL were compared. In the LWIR, T2SL results for R_0A are about 10× below what is theoretically predicted. In the MWIR region the discrepancy is approximately 1000×. T2SL work is concentrated on achieving basic parameters such as R_0A and quantum efficiency. HgCdTe development focus is on operability, uniformity, and the high cost of substrates.

2. IR Material Research at the Army Research Laboratory

The broad range of materials research supported by ARL over the years was reviewed in this keynote presentation, paper -11. III-V materials technology has been one portion of this work, with a focus on both QWIP and T2SL devices. In particular, the ARL spurred the development of corrugated QWIP detectors (C-QWIPs) which are now transitioning to production at L-3 Cincinnati Electronics. Work on MWIR T2SL materials was described, as well as initial efforts to incorporate N and/or Tl into III-V materials, such as InNSb, to create LWIR

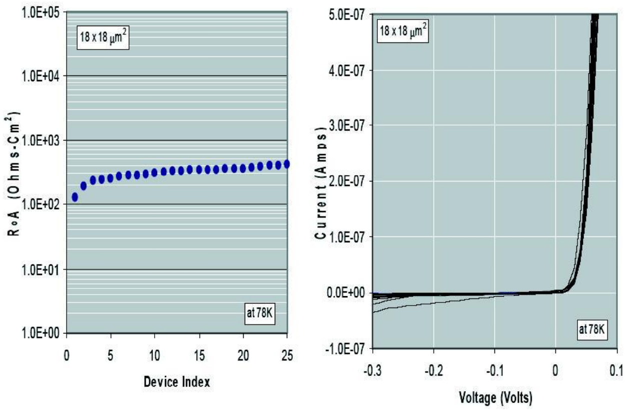

Fig. 4 LWIR (10 μm) HgCdTe detector results on CdTeSe on silicon as described in paper -11. Left, cumulative R_0A product; right, I-V curves at 78 K for 18 μm pixel diodes.

direct bandgap materials. Finally, growth of HgCdTe on silicon was described. Efforts have concentrated on the use of CdTeSe buffer layers with LWIR HgCdTe in an attempt to better match the lattice constants and reduce dislocation densities. Detectors with 10 μm cutoff were fabricated on these substrates by Teledyne and had R_0A median values of 330 Ωcm^2 at 78 K, as illustrated in Fig. 4. Operability of small diodes (18×18 μm) was estimated to be ~99%.

3. HgCdTe detector technology

HgCdTe has established itself as the most versatile detector material for applications that demand the highest performance. It competes with InGaAs in the 1.7 μm spectral range, and InSb in the MWIR, but has no competition today in the LWIR unless requirements are relaxed to allow for low quantum efficiency. Even after nearly 50 years of development, however, there continue to be challenges faced by those using this material. This session addresses several of these issues.

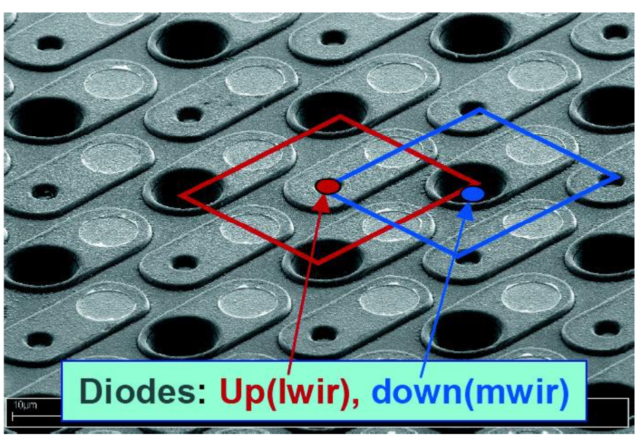

Fig. 5 Psuedo-planar two-color FPAs from Defir have two bumps per pixel on a 30 μm pitch from paper -12.

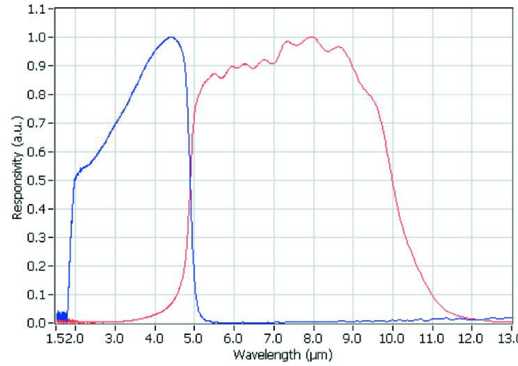

Fig. 6 Psuedo-planar two-color FPA spectral response from Defir, paper -12.

Defir, a joint collaboration between CEA-LETI and Sofradir, led off this session with a description of advanced technology work in paper -12. They first noted that their materials work is now primarily MBE, with two chambers in operation and a third one coming soon that will be capable of growing on 4-inch (100 mm) substrates. For LWIR growth, CdZnTe is used, while Ge is their substrate of choice for SWIR and MWIR applications. Large MWIR arrays, 1280×1024 and 640×512 with 15 μm pixels were described having NEΔTs of 19 mK with 1.2 msec integration time and f/2 coldshields. FPAs have been made with their substrates removed that can detect wavelengths as short as 0.4 μm. LWIR FPAs with formats up to 384×288 and 30 μm pixels are being produced in single-color with ion-implanted n-on-p structures. Two-color devices with one- and two-bumps per pixel have been fabricated. Data was shown for a SWIR/MWIR combination with f/2 NEΔT of 19/15 mK respectively for the two bands. Fig. 5 shows the two-bump pixels used for MWIR/LWIR FPAs, while Fig. 6 shows the spectral response. Lastly, electron avalanche photodiodes have been tested with gains as high as 5300 with 12.5 V bias at 77 K.

Gated diode structures were used in paper -13 to evaluate 1/f noise at the University of Western Australia. The MWIR devices were made using n-on-p structures formed by plasma conversion. The authors found that the noise current, $I_n = \alpha I^{\beta} f^{-0.5}$ trend was observed above 200 pA reverse bias dark current, with $\alpha = 3.5 \times 10^{-5}$ and $\beta = 0.82$.

AIM described the range of HgCdTe detector spectral applications in paper -14, covering SWIR (0.9-2.5 μm), MWIR, LWIR, and VLWIR—13.2 μm at 37 K. Applications included hyperspectral in the SWIR and VLWIR regions, as well as broad-band thermal imaging and seekers in MWIR and LWIR for moderate 384×288 formats. A hyperspectral SWIR format of 1024×256 was reported having a dual-gain CTIA readout with 245 Hz frame rate. The VLWIR hyperspectral detector was made in a 256^2 format and had a frame rate up to 880 Hz for the full format, with higher rates possible for windowed regions. Detailed specifications were presented for the newer SWIR and VLWIR FPAs.

Paper -15, a joint effort of the Army Research Laboratory, EPIR, and DRS, described Auger suppression in LWIR HgCdTe grown by MBE. This effort is aimed at making high operating temperature devices by electrically extracting carriers from the active region of $P^+\pi N^+$ structures. They used a planar three-layer structure and doped the π region by As diffusion. At 300 K the dark current reduction was about 50%.

An MWIR FPA in a 320×256 format with 30 µm pixels was described by the Korean Agency for Defense Development and i3system in paper -119. Responsivity sigma/mean was 3.8%. At f/3.5 a mean NEΔT of 17 mK was measured with a corresponding D* of 6.3×10^{11} Jones. Operability was measured at 99.44% and total power dissipation of the readout with a single output was 33 mW.

Paper -16 from Selex discussed LWIR HgCdTe detectors grown by MOVPE. 10 µm cutoff wavelength layers were grown on 100-oriented GaAs substrates using I as the n-type dopant and As for p-type. Mesa diode structures were fabricated and the substrate was removed. Etch pit density in the range of 10^5 cm^{-2} was measured. Good R_0A was achieved—200 Ωcm^2 at 77 K—see Fig.7. Arrays fabricated in a large format, 640×512 with 24 µm pixels gave an NEΔT <20 mK with f/4 optics and operability of 99.36%.

Plasma etching of HgCdTe was reported in paper -136 from EPIR and NASA Langley. An inductively-coupled plasma was used with a mixture of CH_4, Ar, and H_2 to etch mesas and vias. Various etching parameters were studied with respect to uniformity and roughness of the etched surfaces.

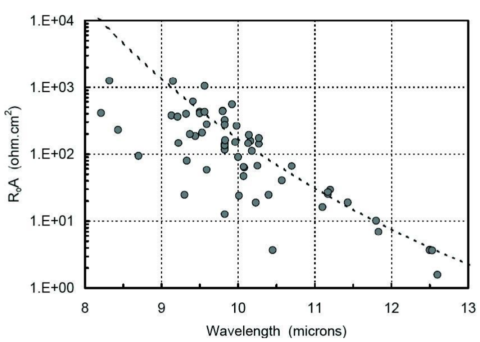

Fig. 7 R_0A vs cutoff wavelength for HgCdTe grown by MOVPE on GaAs substrates described by Selex in paper -16.

4. Short-wave IR FPAs

Development of detectors for the short wavelength infrared (SWIR) band has been very actively pursued for the past several years. They are a potential replacement for image intensifiers under some situations. Other applications in the SWIR include enhanced range for identification and the possibility of range detection through laser radar or range-gated imaging. The SWIR region is also of interest for industrial inspection, fused night vision, and astronomy, including SWIR cameras on the Hubble Space Telescope. Astronomers have an intense interest in the development of large format arrays in this region of the spectrum.

Sensors Unlimited, Goodrich and Valley Oak Semiconductor reported on the performance of SWIR FPAs being developed for photon counting applications in paper -17. 640×512 arrays with 20 µm pixels were built with a variety of readout circuits (two with CTIA, one SFD, and one amplified detector integrator—ADI) to evaluate their performance. Bandwidth was limited to 200 kHz by circuitry in the pixel. Off-chip correlated double-sampling was used. The highest gain CTIA circuit gave the lowest read-noise value of ~9 electrons per pixel per frame.

Low dark current SWIR detectors fabricated with InGaAs diodes was reported in paper -19 by Goodrich. The dark current was reduced to less than 2 nA/cm^2 at a temperature of 12.3 °C. FPAs built with the improved detectors showed improved results over previous iterations of the design. Larger format arrays are planned with this technology.

Paper -21 from the University of Western Australia described progress towards the development of FPAs with pixel-level spectral tunability in the SWIR region. Their approach relies on a Fabry-Pérot cavity suspended on a moveable MEMs structure integrated with a HgCdTe detector. Using a newly-designed, doubly-supported beam they expect to achieve a 60% displacement allowing for tuning from 1.6 to 2.5 µm.

Paper -22 was given by the East China Normal University on the upconversion of SWIR photons to visible-near IR photons. The SWIR wavelengths are those typical of optical fiber communications—1.3 and 1.55 µm. Upconverted photons are in the visible-NIR wavelength range where storage and processing of quantum information can take place such as with Si avalanche photodiodes.

Applications of SWIR detectors are fast increasing. There is a definite need for accurate radiometric characterization of these detectors as well as of systems and scenarios. NIST describes in paper -138 the design of their new high accuracy SWIR radiometer.

5. QDIP FPA advances

Quantum dots provide 3-dimensional confinement of electrons in small regions of one semiconductor material embedded in another. These confined electrons can be photoexcited to produce a photocurrent in the material. A notable property of quantum dots is that normally-incident infrared is absorbed, unlike QWIP stuctures that need mirrors or gratings to deflect the radiation sideways. The three papers in this session reviewed recent work exploring this detector concept.

Paper -23 on two-color QDIP arrays from Taiwan described MWIR/LWIR 256×256 arrays of InAs dots embedded in GaAs. The structure was grown by MBE on 100 GaAs with 30 periods. The spectral response is shown in Fig. 8. A snapshot readout was used. At 80 K the D* was 1.5×10^{10} Jones with 99% operability.

Electric bias was used in paper -24 to control the response of a QDIP detector over the range from SWIR-MWIR-LWIR, as presented by a team from the University of Massachusetts/Lowell and Raytheon. Peak response was seen at 5.6, 7.7, and 10.0 µm and varied as a function of bias. D* as high as 2.3×10^{10} Jones was measured at 78 K.

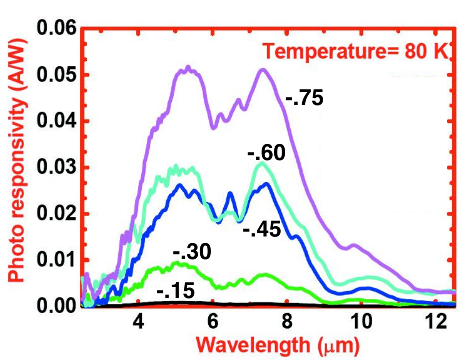

Fig. 8 Spectral response vs. bias from -0.15 to -0.75 V for QDIP detector described in paper -23 shows two wavelength peaks.

Northwestern University reported on self-assembled QDIP arrays in paper -25. MWIR (4.1 µm) devices were built using MOCVD to grow InAs dots and InAlAs barriers on InP substrates. In addition, InGaAs quantum well layers were incorporated into the device. A D* of 2.8×10^{11} Jones was measured at 120 K. Quantum efficiency was reported to be 35%.

6. QWIP FPAs and applications

Quantum-well infrared photodetectors (QWIPs) have demonstrated excellent infrared imagery and can be produced in large format FPAs. Five papers updating developments in this technology were presented.

Paper -26 was presented by the Army Research Laboratory and L-3 Cincinnati Electronics on corrugated QWIPs (C-QWIPs). The corrugated structure provides the orthogonal light coupling to the quantum well layers. Large format arrays are being developed, including 1024×1024 arrays with 25 µm pitch. From test detectors the conversion efficiency was determined to be 6.4% at 5 V bias while the FPA had 2.3% CE. Low NEΔT values of 22 mK at 55 K for a 10.2 µm C-QWIP were reported.

A mega-pixel C-QWIP FPA was reported in paper -27 by NASA Goddard, the Army Research Laboratory, and L-3 Cincinnati Electronics. The array readout has a 1024×1024 format with 25 µm pitch, 8 outputs, 1.3×10^{7} e- storage capacity per pixel, and power dissipation of 220 mW. Fig. 9 shows the spectral response of the FPA.

Thales discussed polarimetric imaging with a QWIP array in paper -28. The array format was 640×512 format with 20 µm pitch. Four linear grating orientations were used on pixel quadrant subarrays to distinguish the polarimetry of the scene, as illustrated in Fig. 10. Po-

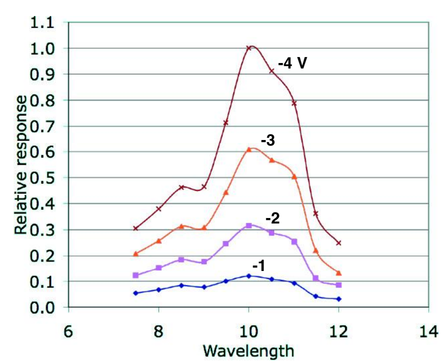

Fig. 9 Spectral response vs. bias from -1 to -4 V of a QWIP FPA from paper -27.

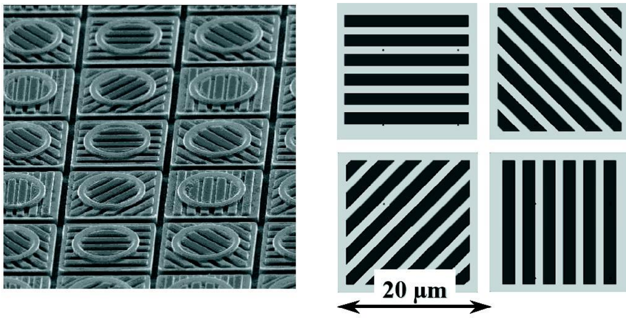

Fig. 10 Layout of linear grating orientations on 4-pixel quadrant subarrays of the QWIP FPA described in paper -28.

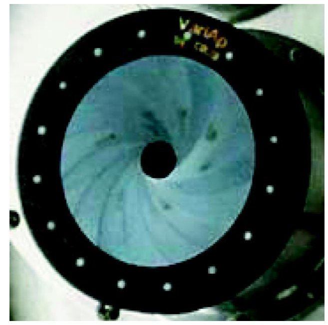

Fig. 11 Variable-aperture cold stop for 3rd generation imagers with variable f/number optics, from paper -32.

larization contrast varied between 35% for vertical and horizontal gratings, and 45% for diagonal gratings.

Paper -29 from IRnova in Sweden described recent advances in their QWIP technology. Two formats have been launched—640×512 and 384×288 both with 25 µm pitch. Increased fill factor and a change in grating allowed the operating temperature to be increased from 65 to 70 K while giving the same NEΔT of 30 mK for f/2.7 and 5 msec integration. Work has begun on smaller pixel sizes and T2SL materials for future LWIR FPAs.

Dual band mega-pixel QWIP FPA development is described in paper -30 from the Jet Propulsion Laboratory, FLIR/Indigo, Air Force Research Laboratory, and the Missile Defense Agency. A combination of MWIR and LWIR response is the goal of this effort. Single color LWIR (16 mK NEΔT with 29 msec integration at 72 K) and MWIR (23 mK NEΔT with 60 msec integration at 90 K) arrays in a 1024×1024 format with 19.5 µm pitch with f/2.5 optics have been demonstrated. Dual band development is being carried out in a 320×256 format with a 40 µm pitch with plans for a 1024×1024 format with 30 µm pitch .

7 and 8. Development of technologies for 3rd generation IR imagers

Third generation detector development has been underway for several years. These sensors are intended to provide enhanced capabilities in future thermal imaging systems, with features such as two-color sensing within each pixel, high frame rates, high temperature operation, active-passive mode combinations, or smart functions that incorporate on-FPA signal processing.

Paper -31 from Thales described two-color QWIP detectors having an extended bandwidth. The first prototype two color QWIP arrays were built in a 384×288 format with 25 µm pixels. Each pixel has two contacts—a common top contact and an individual contact to the intermediate layer between the two QWIP stacks. VLWIR detectors were also reported with a peak response at 14.4 µm.

Variable cold-stop apertures for 3rd generation cameras that operate with more than one f/number were discussed in paper -32 by Opto-Knowledge Systems and White Sands Missile Range. Designs were presented for both existing cameras where an external cold-stop is needed and new systems where the cold-stop can be internal to the detector-dewar. Fig. 11 shows the variable-aperture cold stop.

Paper -117 from QinetiQ gave an update on the development of HgCdTe on Si negative luminescent devices. This technology can be used in 3rd generation systems for variable-aperture cold stops and multi-temperature calibration sources for non-uniformity correction. Winston cone structures improve the device efficiency—see Fig. 12.

MOVPE was used to grow HgCdTe material on GaAs substrates for two- and three-color FPAs as reported by Selex and QinetiQ in paper -33. One-bump mesa diodes were formed and the wavelength was controlled by the bias voltage and polarity. 320×256 arrays with 30 µm

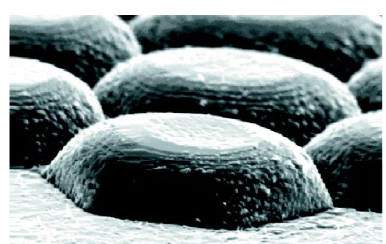

Fig. 12 Etched Winston cone structures improve negative luminescent efficiency as described in paper -117.

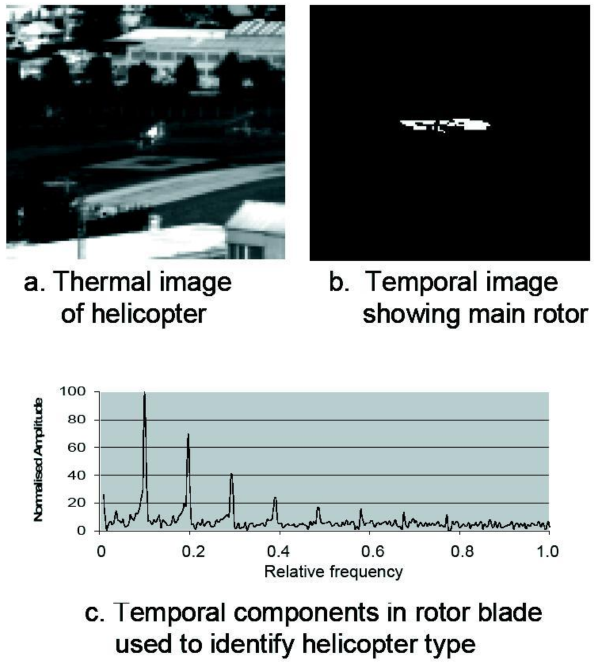

Fig. 13. An example of temporal processing to identify helicopter blades from paper -35.

pixels and hybridized to readouts that had both pMOS and nMOS inputs to accommodate both bias polarities. MWIR/LWIR two-color FPAs had NEΔTs of 12/20 mK for 4/0.08 msec at f/2 with 99.5/97.8% operability, respectively. Experimental 3-color devices were tested.

Numerical analysis by the Military University of Technology, Warsaw of 3-color HgCdTe devices was presented in paper -34. Performance was shown to be critically dependent upon the barrier layers doping level and location relative to the junctions. Several examples were evaluated. Small shifts may result in significant changes in spectral response.

Two types of smart FPAs with on-focal plane signal processing were described in paper -35 by QinetiQ. One of these is used for background pedestal subtraction, allowing for longer integration time and lower NEΔT. The second provides temporal detection to aid in target recognition, as illustrated in Fig. 13 showing the detection of helicopter rotor blades.

Paper -36 discussed techniques for signal preprocessing in variable-acuity sensors. These techniques can be used to reduce the data bandwidth in large format FPAs by estimating activity in the image plane. Important consequences of these techniques lead to reduced data rate coming off the focal plane, resulting in significant savings in power, size, and weight.

9. Development of 3rd generation IR imagers and their technologies

The UK 3rd generation thermal imaging program was reviewed in paper -37 by Selex, QinetiQ, and Thales. It has been given the name Albion—an ancient designation for the UK itself. MOVPE growth on GaAs substrates is being used. An MWIR format of 1024×768 on a 16 μm pitch was chosen to fit existing dewars and to minimize the system cost, but requires dry etching mesas as illustrated in Fig 14. Two LWIR formats are also planned—a microscanned 640×512 FPA format with 24 μm pixels and a high-sensitivity 320×256 with 30 μm pixels which has a smart readout to increase sensitivity (see paper -35).

Paper -38 by Selex summarized signal processor considerations for 3rd generation imagers. These considerations play into the family of cameras described in paper -37. Issues discussed included the modular design of traditional camera functions plus autofocus and microscan capabilities.

Range-gated imaging was the subject of paper -39 by the Swedish Defence Research Agency. This work spans the visible (frequency-doubled Nd:YAG) to 1.57 μm SWIR region. Numerous examples of passive vs. active scene images are given, illustrating many of the phenomena encountered when comparing active to passive imaging, such as imaging through smoke, fire, and water.

DRS reported on 1.57 μm gated imaging with a 128×128 HgCdTe APD array on a 40 μm pitch in paper -40. Their system is built around an MWIR electron avalanche photodiode in HgCdTe that also provides passive imaging from the same sensor. Median gains of ~950 at 11 V bias were measured in the APD mode, with NEPh values of 0.4 photons at 80 K. Gated imagery out to 9 km was obtained. An OPO-converted Nd:YAG laser was used for pulsed illumination.

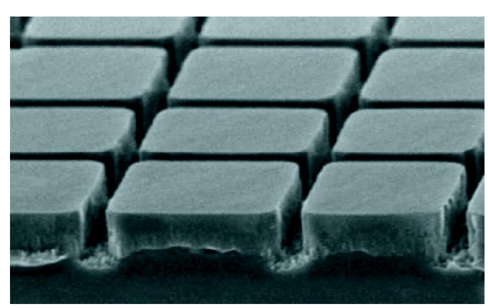

Fig. 14 MWIR HgCdTe pixels with a 16 μm pitch are dry etched to achieve a high fill factor as described in paper -37.

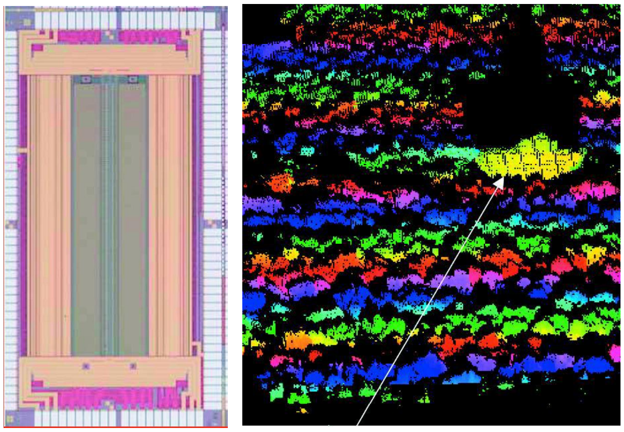

Fig. 15 HgCdTe APD hybrid (left) in a 128×2 linear scanning array operate at room temperature. Right, the arrow points to a 3D image of a tank decoy taken by the Ladar system.

Range-gated imaging performance modeling and simulation was the subject of paper -41 by the Swedish Defence Research Agency. Active imaging provides higher contrast than passive according to the model. Results were compared to experimental data, including factors such as speckle, atmospheric conditions, smoke, image dancing, frame averaging etc.

CEA/LETI reported on electron avalanche photodiodes in HgCdTe in paper -42. MBE was used to grow p-type MWIR layers and diodes were formed on a 30 µm pitch by ion implantation. APD gains up to 5300 at 12.5 V were reported. A bandwidth of 145 MHz was measured at a gain of 5000 giving a gain-bandwidth product of 0.72 THz. An active readout circuit is being developed.

Paper -43 from Raytheon gave an update on p-type avalanche photodiodes. These APDs operate at room temperature. Bandwidths of 1 GHz and noise-equivalent input of 15 photons were reported. Gain uniformity of 3% one-sigma was measured. These devices are being used for single-shot 3D imaging—see Fig. 15.

LWIR (10 µm) HgCdTe detectors with minimal or no cooling were reported in paper -146 by Vigo Systems. Material used in these devices was grown by MOCVD on GaAs substrates. Using optical immersion and 2- or 3-stage TE coolers, responsivities of 5 A/W were achieved together with response speed of 100 psec at a bias of -0.2 V with D* approaching 10^{10} Jones.

IRCAM developed a dual-band (MWIR/LWIR) camera system using QWIP technology as described in paper -141. The format is 384×288 with a 40 µm pitch. A dual field of view lens is provided with 14.6 and 2.8° diagonal FOV. NEΔT is reported to be <30 mK with an integration time less than 10 msec. A variety of output display options are illustrated.

Fig. 16 Microcantilevers with an optical readout produced LWIR images in a 280×240 format as described in paper -45.

10. Novel uncooled technologies I

The papers in this session concern new approaches to making uncooled sensors.

Paper -45 described a bimaterial IR sensor with an optical readout by Agiltron. The sensor was built with a 280×240 format with a frame rate up to and beyond 120 fps and currently has sensitivity of 120 mK at f/1. Fig. 16 shows a representative LWIR image.

Another paper on bimaterial microcantilever pixels with optical readout was reported by Oak Ridge National Laboratory and the University of Tennessee in paper -46. This sensor was built in a 256×256 format. IR images were enhanced with post-processing.

Capacitive readout of bimaterial cantilevers was described in paper –144 by Multispectral Imaging. Fig. 17 shows an SEM of a pixel that has corrugated legs to increase the effective leg length. These are fabricated in a 160×120 format on CMOS circuits capable of sensing

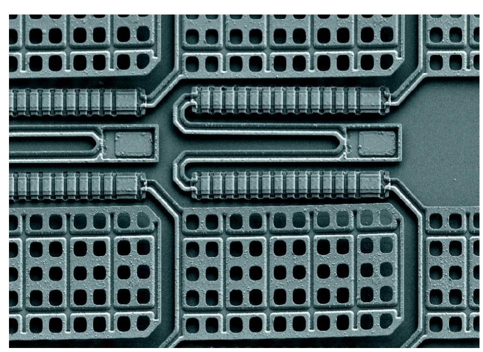

Fig. 17 Bimaterial cantileverer used with a capacitive readout has corrugated legs as described in paper -144.

the change in capacitance as the cantilever moves with changes in the IR flux intensity.

Wavelength selective pixel designs were reviewed by the University of Texas, Foster-Miller, Infoscitex, and the US Army in paper -47. Capacitive-inductive grids provide absorbers that can be tuned to absorb in selective regions of the IR spectrum with the goal of 3-band uncooled FPAs spanning 7-14 µm.

Paper -48 by Nano CVD, Phoenix International, and the University of South Florida addressed dielectric rod antennas coupled to nanoscale metal-insulator-metal tunnel diodes for THz detection. An approach compatible with CMOS foundries was suggested.

11. Keynote session—HgCdTe on low-cost substrates (SWIR to LWIR): opportunities, challenges, and innovations (presentation only)

This keynote presentation by the Army Night Vision and Electronic Sensors Directorate reviewed the motivation and progress towards growing HgCdTe on large area, low-cost substrates. Very good to excellent results have been achieved for SWIR and MWIR wavelength material, with high R_0A products and operability above 99%. For LWIR materials there remain challenges in raising the diode quality and operability—especially high noise tails—of these FPAs. Methodology to evaluate how much of a noise tail may be tolerated while still yielding a useful FPA is being developed in a effort to minimize the cost of future FPAs.

12. Novel uncooled technologies II

Paper -49 presents measurements at IR (10.6 µm) and 2.5 THz frequencies on nanometer-scaled antenna-coupled InGaAs/InP Schottky diodes by Teledyne Scientific, the Florida Institute of Technology, NIST, and the University of Central Florida. E-beam lithography was

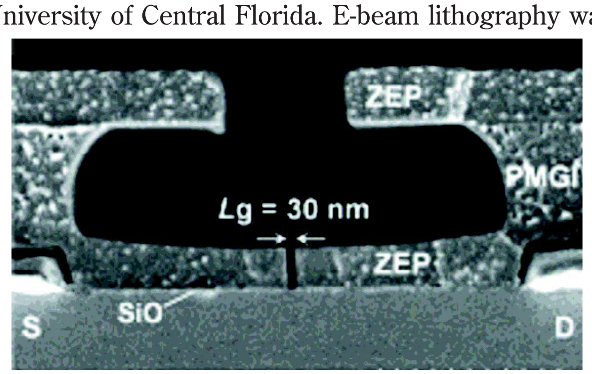

Fig. 18 30 nm gates are defined in InGaAs by e-beam lithography for Schottky diodes as described in paper -49.

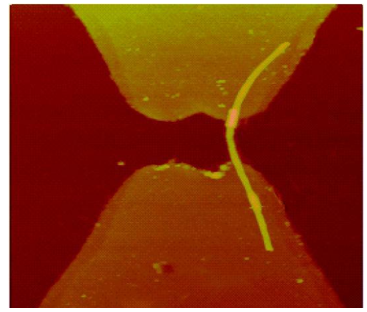
Fig. 19 A semiconducting carbon nanotube has been positioned between electrodes as described in paper -53.

used to make 30 nm gate-length diodes for low capacitance as illustrated in Fig. 18. The diodes were coupled to planar spiral and slot antennas and tested. The estimated D* ranged from 10^4 to $4{\times}10^6$ Jones.

D.C. Sirica gave an update in paper -50 of their approach for an uncooled photon detector using free carriers in a proprietary material incorporating Si particles in a matrix. The concept uses a short wavelength (NIR or visible) to create excited states from which IR photons can be absorbed and free carriers created for detection. The noise sources and project sensitivity of this approach was presented.

A low-cost (100 €) SiGe quantum-well structured bolometer camera for automotive use was the subject of paper -51 by Acreo, the Royal Institute of Technology, Autoliv, Infineon, Umicore, and Vito. This system is intended to be part of an automatic target recognition/avoidance system to avert pedestrian fatalities. The system envisions a small format, 80×30 pixels, camera with a single lens element, with a sensitivity of ~150 mK.

Paper -52 by the Microsystem Technology Group, Royal Institute of Technology, Autoliv, and FAUN addressed some detailed questions about packaging the bolometers described in paper -51 above. Specifically, they believe that the performance margin of the device, partially based on low 1/f noise, will allow packaging without a hard vacuum while still meeting the performance goals of the program.

Carbon nanotubes were evaluated as IR detectors in paper -53 by Michigan State University. These nanometer-sized tubes can allow ballistic transport in direct-bandgap one-dimensional semiconductors. Devices were configured as Schottky diodes and assembled across a pair of electrodes—see Fig. 19. Promising properties for dark current, lifetime, and quantum efficiency were estimated.

The Korean Advanced Institute of Science and Technology described a bimaterial cantilever detector with a capacitive readout in paper -128. Featuring high fill factor, the NEΔT is projected to be <12 mK.

Paper -147 from Redshift described a novel concept of using a temperature sensitive thermal light valve—a diffractive thin film—with an optical readout. Responsivity of 20%/°C were achieved. Low NEΔT and high yield were projected for this device.

13. Uncooled FPAs and applications

Uncooled FPAs are of enormous interest to the community. This session contains papers on this important subject. Tremendous progress has been made since this technology development began in the late 1970s. Today, large-format arrays are available from a number of sources with 25 µm pixels. The trend towards ever-smaller pixels continues as well, along with the drive to add features, reduce cost, and expand applications.

The next generation of security sensors, having a 5× improvement in range sensitivity, based upon modern microbolometers was discussed in paper -55 from Electro-optic Sensor Design. With cost as the major driver small arrays of 10×10 large pixels together with plastic optics are considered. Sensitivity projections of 54 and 140 mK NEΔT are anticipated.

NEC presented the features of 320×240 and 640×480 uncooled modules with a 23.5 µm pitch in paper -56. These units feature dual-gain mode to allow high sensitivity (150°C range with NEΔT ~54 mK) for scene area in the range of ambient temperatures, while also providing the ability to image high temperature objects (540°C range with NEΔT ~140 mK)—see Fig. 20.

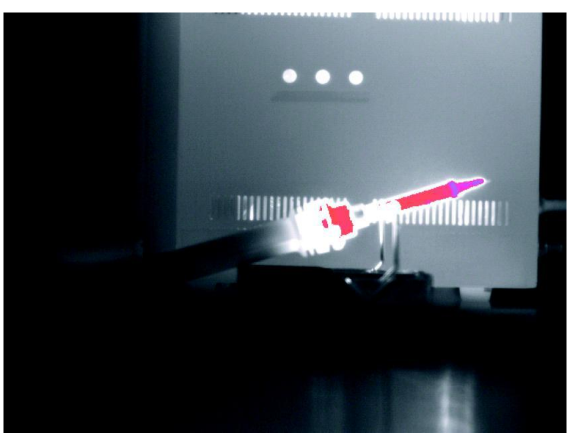

Fig. 20. Both ambient and hot objects can be simultaneously imaged with the dual-range circuitry described in paper -56.

Fig. 21. Imagery from an uncooled 480×640 FPA with 17 µm pixels from paper -59.

Paper -57 by ULIS described efforts to reduce the cost of integrating IRFPAs into cameras. The problem was reported to be due to the dispersion of FPA output signal in the production process. Contributions from the microbolometers themselves (40 mV), but also from the CMOS circuitry (28 mV) were noted. Dispersion of the sigma/mean improved from 1.4% to 1.1% for 160×120 arrays with 35 µm pixels (2004) to 25 µm pixels (2006).

CMOS circuitry that can provide operation of a microbolometer without TE-cooler stabilization was the subject of paper -58 from CEA/LETI and ULIS. The approach is based on the combination of differential reading with the use of reference bolometers and a current mirror circuit.

BAE Systems presented results from their development of 640×480 uncooled FPAs with 17 µm pixels in paper -59. Sample imagery is shown in Fig. 21. Sensitivity at f/1 of 50 mK has been achieved to date. The pixels had a fill factor of 72 % built on a single level.

A 160×120 pixel format on 25 µm centers, amorphous Si microbolometer for high volume applications was the subject of paper -60 from ULIS, IEF-University of Paris Sud, and CEA/LETI. The NEΔT is ≤91 mK for either the analog or digital output mode. The package has no pinch-off tube. A heater is used for temperature stabilization, but the unit can be used with the heater off.

Paper -61 reviewed the design of analog-to-digital conversion in an uncooled microbolometer with a 25 µm pitch. The paper was presented by CEA/LETI and ULIS. Effects of pixel heating from bias were studied. A comparator circuit in the pixel provides digital counts with 14-bit resolution, and the full frame can be integrated.

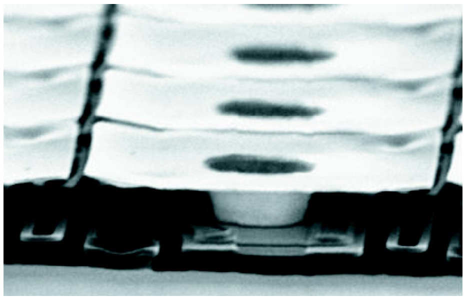

Fig. 22. 17 µm pixel from paper -63 uses a two-level structure to maximize fill factor.

SCD presented paper -62 on medium and large format microbolometers with 25 µm pixels. They have refined the options on their 384×288 format and began testing readouts for a larger, 640×480 format. One variant of the medium format was the ability to operate up to 120 Hz. Evaluation of the use of high-sensitivity arrays with higher f/number optics was made to explore reduced cost.

Paper -63 from DRS reviewed progress on 17 µm pixel uncooled FPA development. A two-layer structure is being used, as illustrated in Fig. 22. Both medium–384×288–and large–640×480–formats have been tested. The medium format array has been developed with options for sensing in the MWIR band and operation up to 120 Hz.

The development progression from 25- to 20- to 17 µm pixels was described in paper -64 by Raytheon—see Fig. 23. All of these have been fabricated in 640×512 and 640×480 formats. Typical average NEΔT of 25 µm pixels was reported to be ~35 mK at f/1 with 12 msec time constant and at 30 Hz.

Polycrystalline PbSe detectors deposited on Si substrates by vapor-phase deposition was reviewed in paper -65 by CIDA and CSIC. The aim of this work is to develop a process to deposit the detectors directly onto CMOS readouts to make low-cost MWIR FPAs for a variety of applications. Work reported in this paper is for a 16×16 array with 200 µm pixels.

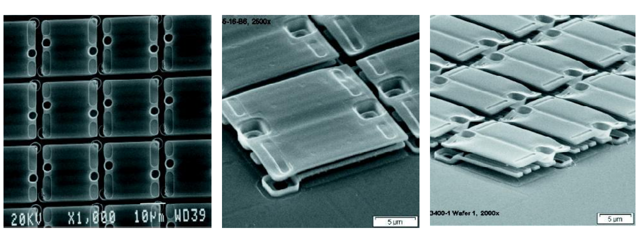

Fig. 23. Left-to-right, 25, 20, and 17 µm two-level pixels from paper -64 shows the evolution of shrinking pixel size.

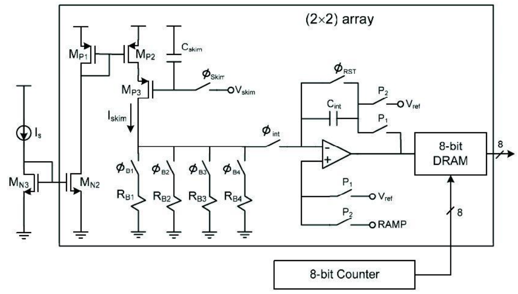

Fig. 24 Circuit diagram of an analog-to-digital converter at the pixel level from paper -66.

Paper -66 describes a pixel-level analog-to-digital converter approach by the Korea Advanced Institute of Science and Technology and the Electronics and Telecommunications Research Institute. One ADC circuit serves a quadrant of four pixels. The circuit diagram is shown in Fig. 24.

An improved method of bias equalization for microbolometers was discussed in paper -132 by the Siberian Branch of the Russian Academy of Sciences. The method involves the substitution of thermally-grounded reference bolometers that do not experience significant heating during a bias pulse with reference bolometers that are not heat sunk but are shielded from the IR radiation.

Fraunhofer addressed the topic microbolometer geometric design in paper -135. They considered amorphous Si material. An optical cavity spacing of 2.1 µm was predicted to be optimum for the LWIR 8-14 µm spectral band. Thermal isolation issues were also discussed.

The topic of uncooled imager's figure of merit was presented in paper -140 by ULIS. The importance of the detector's time constant was noted by comparing two imagers with the same NEΔT × time-constant product.

14. Infrared optics and applications

Infrared imaging requires specialized optical materials. A wide variety of optical components are designed uniquely for the infrared spectral region. This session includes papers on progress in these important technologies.

Umicore presented in paper -67 a new member of their GASIR molded infrared glass family—the GASIR 3—with decreased Ge content. The characteristics of a new coating, which allows the use of GASIR optics in extremely harsh environments, was also described.

Jenoptik addresses in paper -68 the challenges involved in making airborne, high aperture telescopes for surveillance and recognition. They used an iterative combination of manufacturing and measurement techniques for the fabrication of this type of IR optical systems.

Another paper, -69, focusing on light-weight compact optical systems was presented by StingRay Optics. They discussed design considerations directed toward minimizing the weight of the refractive elements as well as of the associated opto-mechanical support housings for thermal imagers on UAV platforms.

Paper -72 was concerned with the use of computational imaging technology in which optics, mechanics, detection and signal processing are jointly optimized, improving the thermal imager's performance beyond what is possible in the optical domain alone. This wavefront coding technique was presented by CDM Optics and illustrated by its use in the design of an LWIR imaging system.

Development of LWIR anti-reflection coatings for HgCdTe space-based imaging devices, which are prone to delamination and degradation due to the extreme environmental conditions, was the topic of paper -73 presented by the Surmet Corporation. This technique, using a physical gradient or motheye structure directly etched into the CdZnTe substrate resulted in excellent broadband performance—see Fig. 25.

Paper -149 in the session demonstrated Melles Griot's new miniature electro-mechanical shutter technology. These shutters, being extremely light weight, having the ability to withstand high vibration and G shock forces and operating reliably in temperature extremes from -40°C to +70°C, provide extended service life to systems like TWS, DVE and UAV.

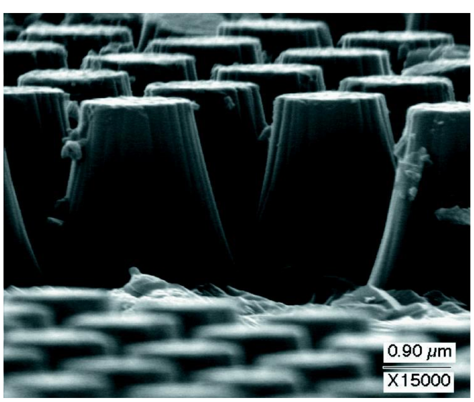

Fig. 25 Motheye antireflection coating on a CdZnTe detector substrate as described in paper -73.

Orion RDE&P Centre discussed in paper -74 the optical and radiometric characteristics of their multispectral thermal imager. The optical filtration is based on multi-beam interference in interferometers positioned at Brewster angle of incidence relative to the imager's optical axis.

Single mode MWIR fibers may be used in countermeasure systems based on heterodyne detection and in IR simulation devices. Paper -148 by Prokhorov General Physics Institute reported on the design, fabrication and optical characterization of step index single-mode micro-structured crystalline optical silver halide fibers. Their optical losses were measured to be 1–2 dB/m and the wide spectral range is 2-20 µm.

15. Cryocoolers for focal plane arrays

Most high-performance infrared photon detectors require cryogenic cooling to reduce thermal-generated noise sources so that photon noise can dominate. This session covers recent developments in this important infrared technology topic.

Ricor reported in presentation -75 on their microminiature cryogenic cooler for portable IR imagers. Among the advantages claimed for their split- linearly-driven cooler are flexibility in system design, long life time, and superior aural stealth. Fig. 26 shows how the power varies with ambient and operating temperature for a 180 mW load.

In paper -76 the same company described their life testing of a one watt linear cryocooler. By running the test 27,500 hours at an elevated ambient temperature of about 70°C an equivalent ambient temperature lifetime of 45,000 hours was estimated for their new linear cryocooler.

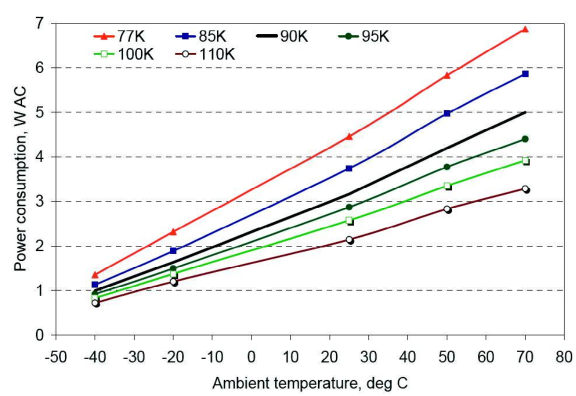

Fig. 26 Linear cooler power consumption as a function of ambient temperature for several operating set points—paper 75.

Raytheon Space and Airborne Systems outlined in paper -77 the design, build and testing of their dual-use long life cryocooler. Dual use refers to the space and tactical cryocooler applications. The company's approach is to modify the mechanical design of the space-cryocooler in order to approach the dual-use cooler.

AIM discussed their moving magnet flexure bearing compressor for split linear coolers. This compressor was designed in order to more than double the cooler's MTTF. Both technical details and performance data for the compressor were reported in presentation -78.

Thales Cryogenics reviewed in presentation -79 the extensions and improvement of their rotary monobloc coolers, linear Stirling coolers and pulse tube coolers.

For Earth observation from a space-based platform the IR systems' FPAs require cooling to a temperature of 40 - 60K. Fig. 27 shows the cooling performance. To achieve this performance Air Liquide DTA, in cooperation with a few other companies and institutions, has developed a large heat lift pulse tube cooler. Its design, manufacture and testing is reported in paper -80.

Ricor suggests in paper -83 the use of an integral digital temperature controller, rather than the traditional analogue version, in miniature Stirling cryogenic refrigerators. The recommendation is based on the fact that the accuracy and stability of the controller's analogue components are not sufficient for the increasing performance demanded from cooled IRFPAs.

In the last of the four Ricor papers, -84, cryocooler selection considerations for an outdoor gamma ray sensor is discussed. This paper is relevant to our IR conference because many of the cooler requirements, like long life, reliability and low vibration signature, are much like those for FPA coolers.

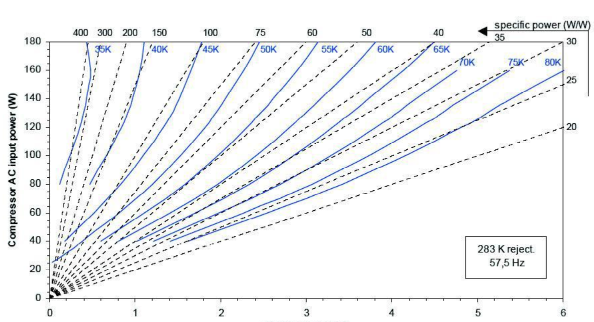

Fig. 27 Space cooler power consumption as a function of cooling capacity for various set points described in paper -80.

16. Vibration control and stabilization in EO equipment

This is a joint session with conference 6569. Only the papers solicited by the session chair belonging to our IR Technology and Applications conference are published in this Proceedings.

Sofradir addresses the requirement on the IR sensor to withstand vibrations and mechanical shocks and thus retain high system performance under severe environmental conditions. In paper -85 they describe their efforts to achieve a more robust Infrared Detector Dewar Cooler Assembly (IDDCA).

Isolation of electro-optic payloads against low frequency vibrations caused by exposure to harsh environmental conditions is the subject of paper -86 presented by Ricor. The authors suggest the use of compliant snubbers to achieve the required payload protection. The optimal snubber design is found by using Ricor's validated analytical model for visco-elastic collisions involving free lumped bodies and snubbers.

Man-portable infrared imagers are sources of audible noise which may give away a soldier's position. In a novel approach Ricor, in paper -88, is effectively attenuating vibration export in the problematic high frequency range by using a special silencing pad while mounting the IDDCA within the imager's housing. Fig. 28 shows the extent of sound reduction achieved.

Pulse tube cryogenic refrigerators do not contain moving mechanical components. Nevertheless, it is known that these types of refrigerators generate vibrations. In their third paper, -90, Ricor discusses experiments designed to identify the sources of these vibrations.

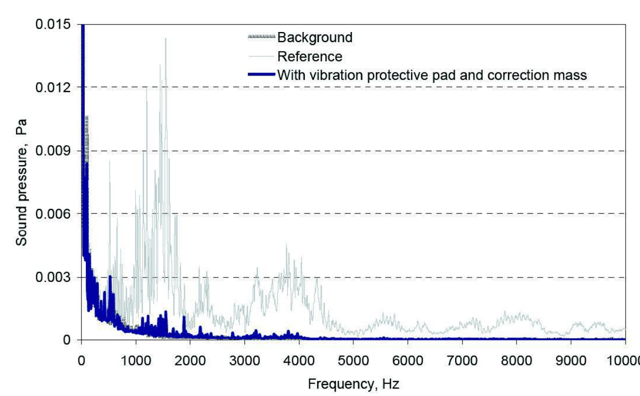

Fig. 28 Vibration reduction from the use of a pad and corrective mass as described in paper -86.

Fig. 29 The concept of the soldier as a system is illustrated above from paper -93.

17. Infrared in future soldier systems

The "Infrared in future soldier systems" session concentrated on formal future soldier programs in a number of countries. These typically include special protective clothing/body armor, network-centric communications and sharing of images, as well as infrared components such as thermal weapon sights, head-mounted sights and handheld sights.

The programs of three countries were reviewed:

- The U.S. Land Warrior and Future Force Warrior programs—which will be fused into the Ground Soldier System (GSS).
- Germany's IdZ
- France's FELIN

Paper -93 was "presentation-only" on the U.S. program. It was presented by the GLJ Group for General Dynamics C4 Systems. The major infrared capabilities of the U.S. program initially include a head-mounted fused (LWIR/low-light-level) sights made by Rockwell-Collins and thermal weapon sights—see Fig. 29.

Papers -94, -95, and -142 on the German IdZ ES ("extended") infantryman of the future program were presented, respectively, by Carl Zeiss Optronics, AIM, and Jena-Optronik. IdZ ES includes:

(1) WBZG - a long range combined reconnaissance and targeting thermal weapon sight for snipers or the squad leader. WBZG is based on AIM's RangIR cooled (MCT) sight. Figure 30 shows HuntIR, on which RangIR is based, in a field exercise.
(2) WBBG - a handheld binocular sight for use by the squad leader. Jena Optronik is lead and using an AIM 384×288 MWIR MCT cooled FPA, CCD visible, LRF (from Zeiss), DMC and wireless link.

Fig. 30 The HuntIR thermal weapons sight in the field—from paper -95.

(3) Video Visor (Videovisier) - a short range uncooled thermal weapon sight for close range applications. It is dedicated for use with assault rifles. Carl Zeiss Optronics is lead.

Papers -97 and -98 (presentation only) by Sagem gave an overview of the French FELIN system, which includes:

(1) Multifunction thermal imagers (binoculars sights based on a 320×240 uncooled microbolometer, eye safe LRF, digital magnetic compass and GPS)
(2) Assault rifle thermal weapon sight - two versions are being made, one with color video and I^2, the other with color video and IR (microbolometer)—Fig. 31.
(3) Light machine gun thermal sight - same as the assault rifle sight with color video and IR (microbolometer), but with longer recognition range.
(4) Sniper rifle sight- direct view video and IR (microbolometer).

18. Infrared search and track (IRST)/target acquisition: systems and technologies I

Infrared provides powerful capabilities for passive searching and tracking that can help detect and keep

Fig. 31 Light machine gun sight with video and infrared microbolometer—from paper -97.

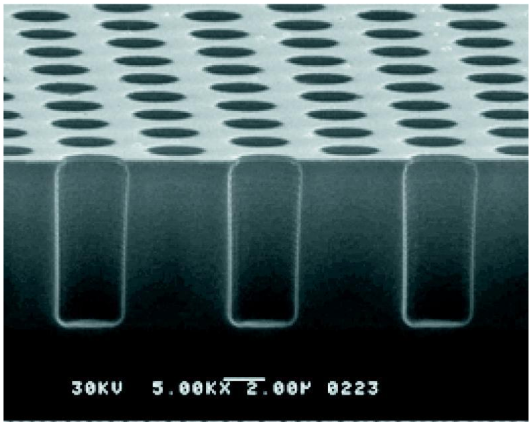

Fig. 32 Structure of a photonic crystal used as an infrared emitter for identification of battlefield friends—see paper -99.

Fig. 33 Image from paper -101 taken with a 640×512 InSb camera with 15 µm pixels and f/4 optics.

awareness of the location of adversaries in the field. Session 18 and 19 provide updates in this field of infrared technology applications.

Avoiding friendly fire in the battlefield is a critical issue facing the Army. Ion Optics demonstrates in paper -99 their Identify Friend or Foe (IFF) system based on photonic crystal enhanced emitter technology—see Fig. 32. Viewing distances of above 500 m and 5 miles were reported for ground-to-ground and ground-to-air prototypes, respectively.

Improved situational awareness near the coast (the littoral) in operations against international terrorism and in asymmetric warfare are issues of major concern to the Navy. The Dutch TNO institute reviewed in paper -100 their approaches to design and performance assessment of systems concepts for future IRST development. Focus is set on the importance of smart signal processing.

19. Infrared search and track (IRST)/target acquisition: systems and technologies II

SCD, SemiConductor Devices, described their new Pelican 640×512 pixel InSb detector family in paper -101. Due to its small 15 µm pitch this FPA fits into mid format dewars and thus enable upgrading of mid-format systems to higher spatial resolution—see Fig. 33.

In paper -103 Elta presented their staring IRST system for airborne and naval applications. The system employs a multispectral technique for target verification over a 360° horizontal field of regard. Continuous scanning coupled with a counter-rotator accounts for the staring action.

The technologies used in the design of Thales' Distributed Aperture System, DAS, type IRST were the subject for presentation in paper -104. The design drivers and their original optical design were discussed in some detail.

In another paper, -127, by the Thales group the applications of their Catherine–XP thermal imager is reviewed. This compact system is based on Sofradir's TV/4 format LW 384×288 QWIP FPA with a 25 µm pitch. New developments like dual-band operation and polarimetric imaging were outlined.

SWAD, a detection and warning system against multiple small arms fire, was proposed by Elisra Electronic Systems in paper -107. The system, having a wide field of view and a high frame rate, detects the firing at hundreds of meters and transfers the source coordinates to their own forces.

TANDIR, another of Elisra Electronics Systems' warning devices, was presented in paper -108. Its design incorporates a 320×640 pixels 60 Hz uncooled LWIR bolometer and is optimized for detection of ATGMs. Clutter rejection is based on recognition of the threat's temporal profile.

Paper -109 was concerned with the optronic sensors for LFK-MBDA's new firing post designed for the upgraded Milan anti-tank missile system. The post is equipped with a wide FOV CMOS based tracking sensor. The missile's position and a thermal image of the scene are projected into a sighting channel via a multi-spectral projector.

Optigo Systems demonstrated in paper -110 the performance of their Transient Event Detector, TED, system in the laboratory and under field conditions. Architecture and design concepts were presented for this type of miniaturized, wide FOV detection and situation awareness system.

In a second paper, -111, LFK-MBDA outlined their design concept and expected performance of a semi-active/passive dual-mode seeker capable of autonomous operation in beyond-line-of-sight missions. The final system is expected to operate with a laser target designator and an imager based on a microbolometer FPA. The lab and field performance of a demonstration model, having the thermal imager replaced by a TV, was shown.

A novel adaptive algorithm for detection by IRST systems of targets in clutter was proposed in paper -134 by Kyungpook National University and South Korea's Agency for Defense Development. The algorithm, which is based on a detection index using the local gamma correction and target motion information, was successfully applied to IR images of distant aircraft.

20. Selected application presentations

Unencumbered operation of critical infrastructure systems necessitate comprehensive detection, management and control systems. L-3 Infrared Products illustrated, through case studies in paper -130, applications of thermal imaging by first responders in homeland disaster situations where reliable detection and situational awareness are critical issues.

In a related presentation, paper -113, Mine Safety Appliances concentrated on a specific group of first responders – the Firefighters. The Thermal Imaging Camera (TIC) is an accepted mission critical tool for firefighters. The impact on the IR sensor industry from the need for better image quality, Fire TIC Standard, durability and ruggedness metrics, as well as standard testing methods were reviewed.

Microspectrometers consisting of a Fabry-Pérot filter integrated directly on a HgCdTe detector enable rapidly tunable hyperspectral IR-FPA imagers. University of Western Australia (paper -114) presented measured results and discussed design issues for MEMs based microspectrometers operating in the SWIR and MWIR spectral regions with linewidths of 55 nm and 210 nm, respectively. Fig. 34 shows the MEMs structure.

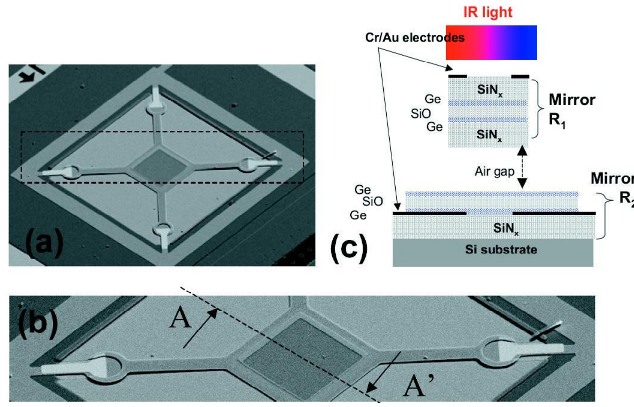

Fig. 34 MEMs Fabry-Pérot filter for hyperspectral imaging as described in paper -114.

The Space Science and Engineering Center of University of Wisconsinn-Madison reported in paper -115 on their IRCIR payload for global measurements of ice water in the atmosphere. The measurement system's baseline design was outlined. It is a compact, multispectral, wide FOV pushbroom IR imaging radiometer with four uncooled microbolometer FPA sensor assemblies which produce 90° cross-track coverage in three spectral bands—see Fig. 35.

Ice forming on the cryogenic-filled Space-Shuttle's external tank is a potential threat to vehicle and its crew. The U.S. Army described in paper -116 their mobile NIR ice detection and measurement system developed by MDA of Canada and tested in cooperation with NASA. It was shown that the pre-launch inspection system has the capability to remotely detect and measure ice layers of 0.25 inch thickness.

Paper -137 by University of Puerto Rico-Mayaguez relates to remote detection of concealed explosives. It was demonstrated that Fiber Optic Grazing-angle Fourier Transform IR Reflection-Absorption Spectroscopy

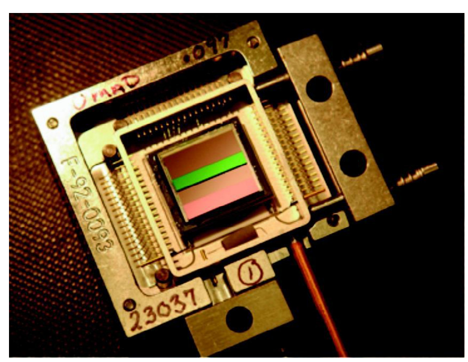

Fig. 35 Radiometer focal plane with striped filters for cloud ice measurements as described in paper -115.

can be used as a surface analyzer for detecting nitro explosives such as TNT on plastic surfaces. Airport screening was suggested as a potential application of the technique.

Paper -139 is a follow-on to paper -137. In the present study the detection of several explosives was carried out while the explosives were smeared on stainless steel sheets.

21. Selected technology presentations

Systems designed for certain strategic applications have severe constraints on excess low frequency noise due to the effect the noise has on image uniformity with subsequent consequences on the period of calibration. DRS Sensors & Targeting Systems presented in paper -118 data and analysis of excess low frequency noise in LWIR HgCdTe High Density Vertically Integrated Photodiode detectors.

SemiConductor Devices, SCD, has measured the 2-D spatial response of individual elements in their 30, 20 and 15 μm pitch InSb FPAs. Two measurement methods were used and the results, reported in paper -120, showed good agreement with the outcome of a numerical simulation. The data is used for estimation of MTF and crosstalk.

CEA/LETI suggests in paper -121 that σ–δ A/D converters are promising for high performance and medium size cooled FPAs. A column level ADC demonstrator is presented and its performance is reported together with perspectives for future developments.

Gas cluster ion-beam etching of InSb substrates was the subject of paper -131 by Galaxy Compound Semiconductor and five additional organizations. Use of this method, as opposed to chemical-mechanical polishing, may preclude the need for additional etching before MBE growth.

22. ROIC and Non-Uniformity Correction

Sofradir is presenting in paper -124 the results of their effort to reduce the non-uniformity in their HgCdTe FPAs. Their success, based on improved wafer layer homogeneity and readout circuit linearity, has led to reduced calibration constraints and optimized image quality over a wide range of operating conditions.

L-3 is demonstrating in paper -125 the advantages of their improved scene-based Non-Uniformity Correction, NUC, technique. Standard scene-based NUC approaches can at times introduce image artifacts. The proposed technique avoids these artifacts by incorporating a correction term for each element into the algorithm. This term is based on motion estimation and texture segmentation.

Researchers from Universidad de Concepcion in Chile, joined by U.S. and Chinese groups, present in paper -126 a new scene-based non-uniformity correction technique which is based on a noise correction system that compensates for bias non-uniformity. Good results are claimed, albeit with some ghosting artifacts.

The Middle East Technical University is proposing in paper -145 a non-uniformity correction technique for microbolometer FPAs that is based on changing the detector temperature by use of bias heating prior to the readout phase. It is claimed that this correction method leads to smaller readout circuits, lower noise floor and less power dissipation.

Paper -133 from the Korean Advanced Institute of Science and Technology discussed a readout circuit design for Time-Delay-and-Integration (TDI) for satellite sensor applicaitons. A circuit using an adaptive charge capacity changing method was analyzed.

Paul R. Norton
Bjørn F. Andresen
Gabor F. Fulop